TELKOMNIKA Telecommunication Computing Electronics and Control
Vol. 21, No. 3, June 2023, pp. 649~656
ISSN: 1693-6930, DOI: 10.12928/TELKOMNIKA.v21i3.24749

Using phosphor $ZnB_2O_4:Mn^{2+}$ for enhancing the illuminating beam and hue standard in white light-emitting diodes

Ha Thanh Tung[1], Huu Phuc Dang[2]
[1]Faculty of Basic Sciences, Vinh Long University of Technology Education, Vinh Long Province, Vietnam
[2]Faculty of Fundamental Science, Industrial University of Ho Chi Minh City, Ho Chi Minh City, Vietnam

Article Info

Article history:

Received Dec 01, 2022
Revised Dec 30, 2022
Accepted Jan 10, 2023

Keywords:

Color rendering index
Luminous efficacy
Mie-scattering theory
Phosphor geometries
$ZnB_2O_4:Mn^{2+}$ green phosphor

ABSTRACT

The enhancement in hue uniformity and luminous production of multiple-chip white LED lamps (MCW-LEDs) using dual-layer remote phosphor packaging designs are the emphases of this paper. We blended Mn^{2+} activated strontium–barium silicate ($ZnB_2O_4:Mn^{2+}$) with the phosphor mixture and manage to record significant impacts of this new phosphor mixture on the LED lights' lighting performance. There is evidence that the growing concentration of yellow-green-emitting $ZnB_2O_4:Mn^{2+}$ phosphor encourages the enhancement of hue uniformity and illumination effectiveness in MCW-LEDs with mean correlated hue heats (CCTs) of roughly 8500 K, though the color quality scale is gradually deteriorating. It is possible to successfully achieve such amazing MCW-LED performance if we choose the right concentration and size of $ZnB_2O_4:Mn^{2+}$.

Corresponding Author:

Huu Phuc Dang
Faculty of Fundamental Science, Industrial University of Ho Chi Minh City
No. 12 Nguyen Van Bao Street, Ho Chi Minh City, Vietnam
Email: danghuuphuc@iuh.edu.vn

1. INTRODUCTION

Lately, white light emitting diodes (WLEDs) have gotten huge amounts of notice in the illumination industry owing to their excellent performance and extended lifetime. Typically, they have two designs for general illumination. The first form is to excite the yellow phosphor with an InGaN light emitting diode (LED) chip in blue and mix the blue and yellow illumination with white illumination. The second one mixes various monochromatic lights by using various chips to produce white light, which is also a complicated and expensive method. Under those circumstances, the most cost-effective and power-efficient approach to manufacturing white light is to use phosphor conversion materials [1]-[3]. Yttrium garnet yellow phosphor ($YAG:Ce^{3+}$) is now the most frequently utilized and good-grown transformation substance $YAG:Ce^{3+}$ offers many benefits, such as excellent blue illumination absorption and exceptionally effective emitting procedures with a quantum productivity of around 90% [4]-[6]. Due to the shortage of red light components and poor color coordinates, the $YAG:Ce^{3+}$ activated using the InGaN chip only produces white illumination spectrum with low color rendering index (CRI) of less than 80. The most possible and potential option to make WLEDs that offer higher CRI is to combine the red and yellow phosphors. However, the growth of high CRI WLEDs is restricted due to the poor effectiveness of red phosphors [7]-[9]. The photoluminescence quantum yield (PLQY) of semiconductor quantum dots (QDs) is high; and they also have a broad absorption spectrum, low scattering impact, size-adjustable emission, good color saturation, and strong photo-oxidation resistance [10]-[13]. In that case, substituting the phosphor with QDs substance would be one effectual way to generate white illumination. When changing the bandgap, CdSe QDs can release a whole observable band of color [14]-[16]. Jiang *et al*. [17] created WLED devices yielding a CRI value reaching 76 using an InGaN chip for the task of stimulating several distinct magnitudes for CdSe/ZnS QDs in 2008. Keshri *et al*. [18] developed mixture WLED devices with core/shell CdSe NCs implemented above InGaN/GaN LED yielding hue coordinates shown as (0.356, 0.330) and a CRI value of 87.4. During the identical period, Xi *et al*. [19] also developed CdSe/CdS/ZnS core/multi-shell QDs that created a merger between green, yellow, red emitting QDs, epoxy compounds and InGaN LED components. The manufactured International Commission on Illumination (CIE) chromaticity coordinates of the white LEDs are (0.35, 0.37) and the CRI is 88. Despite its superb fluorescence properties and promising utilization in the production of white LEDs, cadmium (Cd) in QDs is a poisonous metal. Therefore, the application is not eco-friendly, and substitution is required. Research showed that WLEDs constructed combining InP QDs and phosphorescence have the ability to reduce red spectrum faults and increase color rendering performance. However, it is somehow complicated to fabricate the new LED devices utilizing QDs since it requires a much smaller size in comparison to the other materials.

The conventional phosphors present broad emission ranges and thus causing energy inefficiency. Therefore, the phosphor with the narrow emission band turns out to be more favorable, in terms of fabricating the LED with improved optical and energy efficiencies. Here, we decided to select the $ZnB_2O_4:Mn^{2+}$ green phosphor for the research of enhancing the color quality and luminous efficacy of phosphor-converted LED packages. The $ZnB_2O_4:Mn^{2+}$ is a phosphor that emits a strait emission range with the peak radiation at 541 nm. Research previously showed that it possesses a broad band of excitation of 235 nm – 535 nm that is significantly strong in the blue-light wavelength band. Thus, this $ZnB_2O_4:Mn^{2+}$ is suitable for combining with blue LED chips to produce white lights. Moreover, the thermal and color stability of this green phosphor is also excellent [20], [21]. Also, this study analyzes the optical impacts of $ZnB_2O_4:Mn^{2+}$ green phosphor on the two lighting aspects of color and luminescence performances of WLEDs. The phosphor packaging structures needed for the research are the conformal coating, the in-cup, and remote phosphor configurations, as they are the popular methods of creating a phosphor-converted WLED. Consequently, based on the attained results in this study, we can affirm that it is possible to choose green phosphor $ZnB_2O_4:Mn^{2+}$ to acquire the improved performance of all three phosphor packaging structures.

2. PREPARATION AND SIMULATION

2.1. Making $ZnB_2O_4:Mn^{2+}$

Phosphor $ZnB_2O_4:Mn^{2+}$ is an indispensable part in this article. Therefore, for the task of obtaining the greatest phosphor films capable of yielding particular outcomes, it is vital to appropriately produce the phosphor substance. As seen in Table 1, $ZnB_2O_4:Mn^{2+}$ is made up of three separate elements. It's a three-stage heating process. For the task of obtaining a stable blend, every component is dry milled or ground prior to the initial phase. Then, under a temperature around 500 ˚C, the blend will be heated within open quartz boats. Bring this combination out afterwards and powder it with the milling process. The second stage of fire follows. Throughout 1 hour, the powdered material is heated again at 700 ˚C within open quartz boats. After this stage, the substance will undergo further powdering process. Afterward, the final fire stage will take place in the similar container as the earlier ones, however this time the burning heat will be 1300 ˚C and the firing period will be 2 hours. As expected, the results should have these optical properties emitting highest point of 2.29 eV, and emitting broadness (FWHM) of 0.21 eV. As a matter of fact, the stimulation effectiveness by UV would show − (4.88 eV), – (3.40 eV), and +/4–5% by e-ray. Finally, it would be necessary to be exponential decay, roughly 26 msec to 1/10 [20], [21].

Table 1. Ingredients for $ZnB_2O_4:Mn^{2+}$

Ingredients	Mole (%)	By weight (g)
ZnO	97	79
$MnCO_3$	3	3.5
H_3BO_3	205	127

2.2. Building MC-WLED device

As reported by the Monte Carlo method and LightTools 9.0 application, the actual phosphor film of multiple-chip white LEDs (MCW-LEDs) is replicated with a plain silicone film. This modeling technique is comprised of two different phases: 1) determining and producing mechanical constructions and optical qualities of MCW-LED lamps, and 2) carefully monitoring optical effects of phosphor compounding within the wide range of $ZnB_2O_4:Mn^{2+}$ concentrations. We must conduct some comparisons so as to comprehend the compounding influence from $YAG:Ce^{3+}$ as well as $ZnB_2O_4:Mn^{2+}$ imposed on the productivity for the MCW-LED device. The phosphor composition is applied to the three WLED structures with a mean correlated chroma temperature (CCT) of 8500 K, including protective-coating, in-cup, and remote phosphor structures. An actual MCW-LED lamp daubed in phosphor compounding under median CCT measured at 8500 K is well-defined via Figure 1(a), while its details are displayed by Figure 1(b). It also denotes the simulation of MCW-LEDs without the presence of ZnB_2O_4:Mn^{2+}. The reflector's bottom longitude would be measured at 8 mm, the altitude would be measured at 2.07 mm, with the peak exterior length reaching 9.85 mm. Nine chips will be daubed in the conformal phosphor compounding, which is 0.08 mm thick. Each chip is square, reaches 1.14 nm in length, has an altitude reaching 0.15 mm and would be linked to the reflector's gap. The chips' peak wavelength reach 453 nm, its radiation is 1.16 W. Figures 1(c), Figure 1(d), and Figure 1(e) demonstrate three distinct phosphor structures of protective-coating phosphor (CP), in-cup phosphor (IP), as well as distant phosphor (RP), respectively. Aside from that, the phosphors are combined with the silicone matrix to form the phosphor layers. For this reason, all structures utilize Mie hypothesis for the task of examining the dispersion for granules of phosphor. The average diameter for all phosphor particles according to this article is 14.5 μm, the same as the real phosphor particle size.

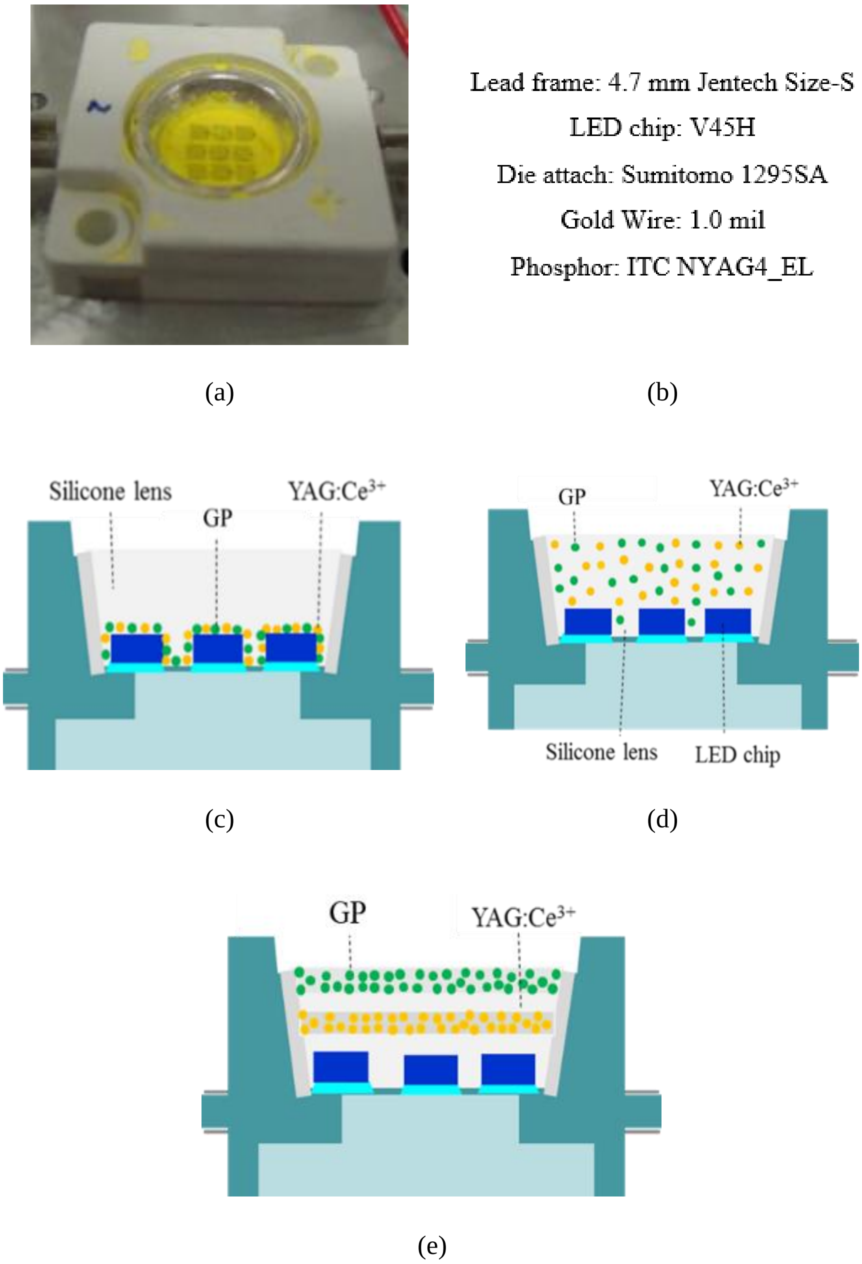

Figure 1. Picture detailing phosphor-transformed MCW-LED device with doped ZnB_2O_4:Mn^{2+}: (a) the employed device, (b) technical parameters, (c) protective-coating phosphor, (d) in-cup phosphor, and (e) distant phosphor

$ZnB_2O_4:Mn^{2+}$ particles, $YAG:Ce^{3+}$ granules along with silicone make up the phosphor compounding. The refractive indexes of $ZnB_2O_4:Mn^{2+}$, $YAG:Ce^{3+}$, and its silicone would be 1.85, 1.83, and 1.52, in turn, and their sizes are similar with the real values. The emission spectra of the prepared phosphor compound can be obtained following the assessment of the refractive index as well as particle magnitudes for the phosphor. Figure 2 illustrates various $ZnB_2O_4:Mn^{2+}$ concentrations with the emitting spectra of the phosphor geometries. In the conformal structures, the concentration of $ZnB_2O_4:Mn^{2+}$ is from 0% wt to 24% wt, see Figure 2(a). Judging Figure 2(b) and Figure 2(c), the $ZnB_2O_4:Mn^{2+}$ concentration ranges in the in-cup and remote configurations are 0% – 1.4% wt and 0% – 20% wt, respectively. The lumen outcome of MCW-LEDs will expand since $ZnB_2O_4:Mn^{2+}$ particles are applied to the phosphor compound, as can be seen in these graphs.

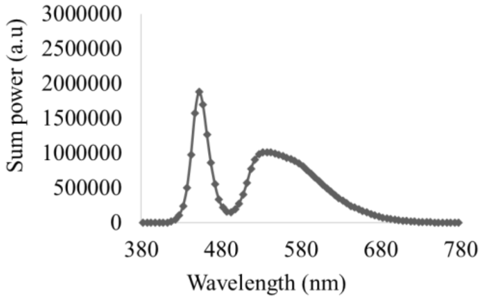

(a)

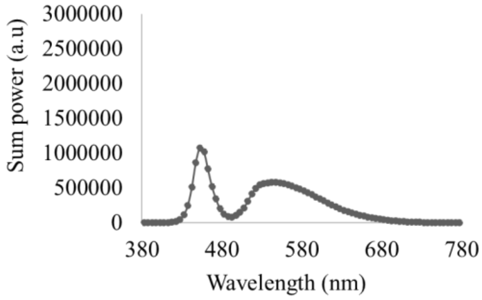

(b)

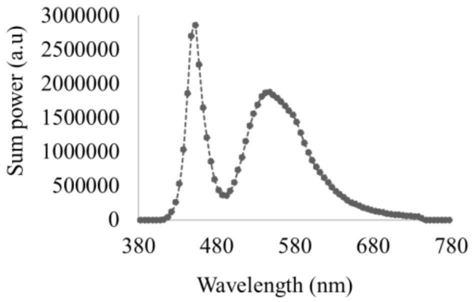

(c)

Figure 2. Discharge spectra in several phosphors: (a) CP, (b) IP, and (c) RP

3. RESULTS AND DISCUSSION

Conforming to the Mie theory [22]-[25], the dispersing factor μ_{sca} is determined to check the light features in phosphor composition. The following expressions will assess the correlation concerning the dispersing factor (SC) as well as the wavelength counting the size of $ZnB_2O_4:Mn^{2+}$ particles:

$$\mu_{sca}(\lambda) = \frac{c}{\bar{m}} \bar{C}_{sca}(\lambda) \tag{1}$$

$$\bar{C}_{sca}(\lambda) = \frac{\int C_{sca,D}(\lambda) f(D) dD}{\int f(D) dD} \tag{2}$$

$$\bar{m} = \frac{\int m_i(D) f(D) dD}{\int f(D) dD} \tag{3}$$

$$C_{sca}(\lambda) = \frac{P_{sca}(\lambda)}{I_{inc}(\lambda)} \tag{4}$$

$C_{sca,D}$ represents the dispersing cross-section in the phosphor possessing granule diameter D. $f(D)$ indicates the magnitude dispensation function. c indicates the phosphor dosage (g/cm^3). While $\bar{C}_{sca}(\lambda)$ and $\bar{m}$ will be the dispersing cross-section and granule weight for the phosphor, respectively, implemented into $f(D)$. The dispersed energy for granules as well as the irradiance strength, are $P_{sca}(\lambda)$ and $I_{inc}(\lambda)$.

Figure 3 chronicles the dispersion coefficient (SC) for sheet of phosphor when $ZnB_2O_4:Mn^{2+}$ phosphor is present. It is clear that changing $ZnB_2O_4:Mn^{2+}$ concentrations will cause the SC of the phosphor combination to fluctuate significantly, see Figure 3(a). It also proves that the pre-stimulus and intensity of $ZnB_2O_4:Mn^{2+}$ influence the color quality of CP and IP structures. Despite $ZnB_2O_4:Mn^{2+}$ particle size, SC seems to amplify when the concentration of $ZnB_2O_4:Mn^{2+}$ rises, as shown in Figure 3(b). Moreover, SC increases dramatically at a particle size of around 1 µm than at bigger size, leading to the hue uniformity development. Occasionally, if we aim for chroma quality scale (CQS), the size of the $ZnB_2O_4:Mn^{2+}$ can be around 1 µm. The SC factor of the phosphor film grows stably when its size is about 7 µm, notwithstanding its heightened concentration. This event will advance the hue standard (CQS) of LEDs tremendously. Subsequently, the smaller size of 7 µm can be a suitable option if the objective is CQS. The SC factor is undoubtedly dependent on both the dosage and the size of $ZnB_2O_4:Mn^{2+}$. This is why $ZnB_2O_4:Mn^{2+}$ can be a potential to enhance the lumen performance as well as hue consistency for LED device.

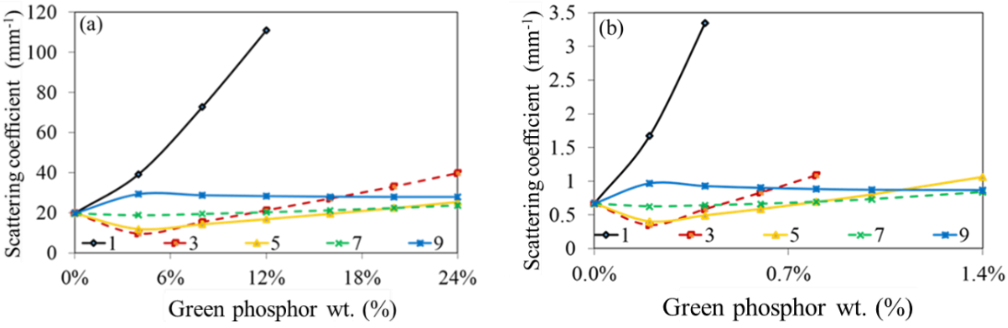

(a) (b)

Figure 3. Dispersing factors for phosphor composition under 453 nm correlating with the dosage as well as magnitude for $ZnB_2O_4:Mn^{2+}$: (a) CP and (b) IP

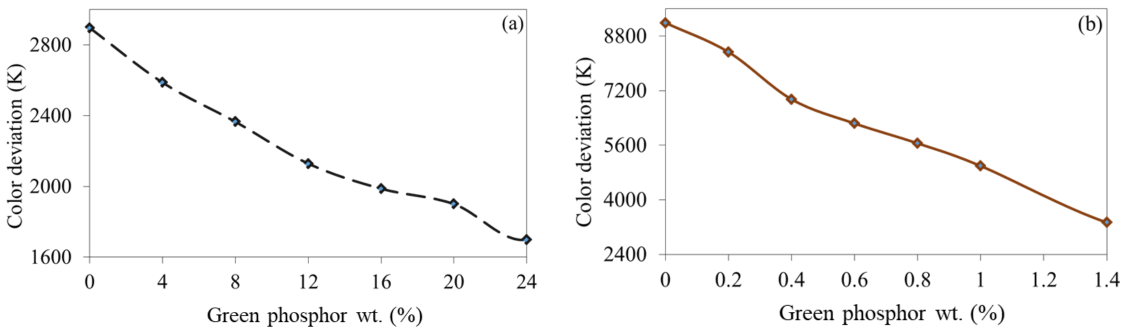

(a) (b)

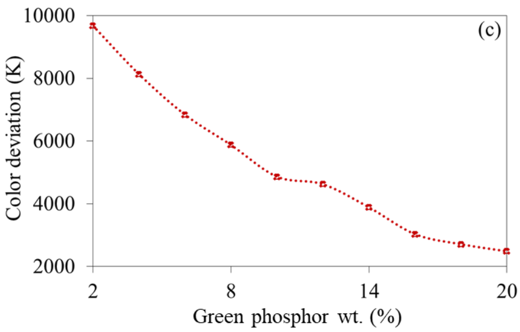

(c)

Figure 4. The CCT aberration correlating with the dosage as well as magnitude of $ZnB_2O_4:Mn^{2+}$: (a) CP, (b) IP, and (c) RP

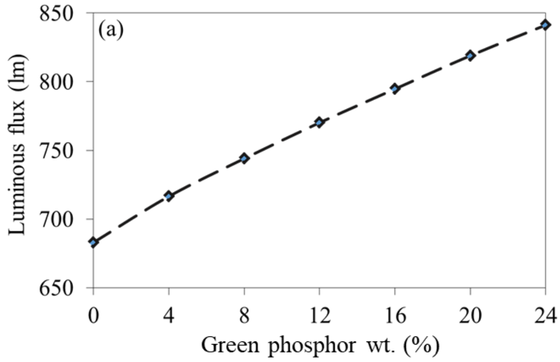

(a)

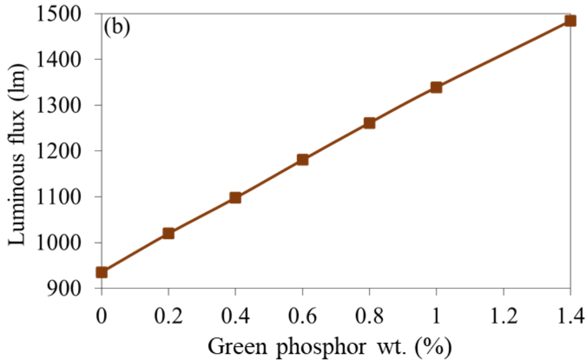

(b)

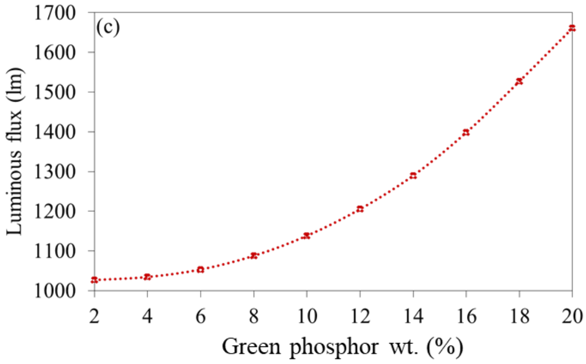

(c)

Figure 5. Illuminating effectiveness correlating with the dosage as well as magnitude for $ZnB_2O_4:Mn^{2+}$: (a) CP, (b) IP, and (c) RP

In this post, it is meaningful that meeting the LED product's specifications is critical, especially in our study, MCW-LED inquiries average CCT of 8500 K. Because of the sustained CCT of 8500 K, it is vital to reduce the $YAG:Ce^{3+}$ phosphor considerably when the dosage for $ZnB_2O_4:Mn^{2+}$ phosphor increases. The following formula can reckon the heaviness ratio of the LED phosphor film:

$$W_{sil} + W_{yp} + W_{gp} = 100\% \tag{5}$$

In this formula W_{sil}, W_{yp}, and W_{gp} are the heaviness percentages of the silicone, $YAG:Ce^{3+}$, and $ZnB_2O_4:Mn^{2+}$ in turn.

As demonstrated in Figure 4, the angular hue for aberration for MCW-LED device is dependent on the presence as well as the lack of $ZnB_2O_4:Mn^{2+}$ in the simulation. In particular, the color variations become smaller as the dosage of $ZnB_2O_4:Mn^{2+}$ green phosphor grows, regardless of the applied structures, see Figure 4(a). In other words, with the addition of $ZnB_2O_4:Mn^{2+}$, the peak-valley deviation of the CCT is greatly reduced, as shown in Figure 4(b) and Figure 4(c). Figure 5 displays illuminating effectiveness correlating with the dosage as well as magnitude for $ZnB_2O_4:Mn^{2+}$. Similarly, compared to MCW-LEDs without $ZnB_2O_4:Mn^{2+}$, the spatial hue dispensation of MCW-LEDs with $ZnB_2O_4:Mn^{2+}$ is substantially flatter, see Figure 5(a). Ideally, if we can balance the two performance criteria, the optimization problem can be solved. Yet, in fact, if we simply improve one factor, the optical system will suffer in other regions, and the expected CQS factors and the performances of the white LED packet are unobtainable at the similar period, see Figure 5(b). If we want to have a good CRI, the solution is to maximize the broad source spectrum and heighten the efficiency with monochromatic radiation's wavelength at 555 nm. According to this investigation, color quality scale (CQS), illuminating beam, as well as CCT P-V aberration factors would be notable features, as displayed in Figure 5(c).

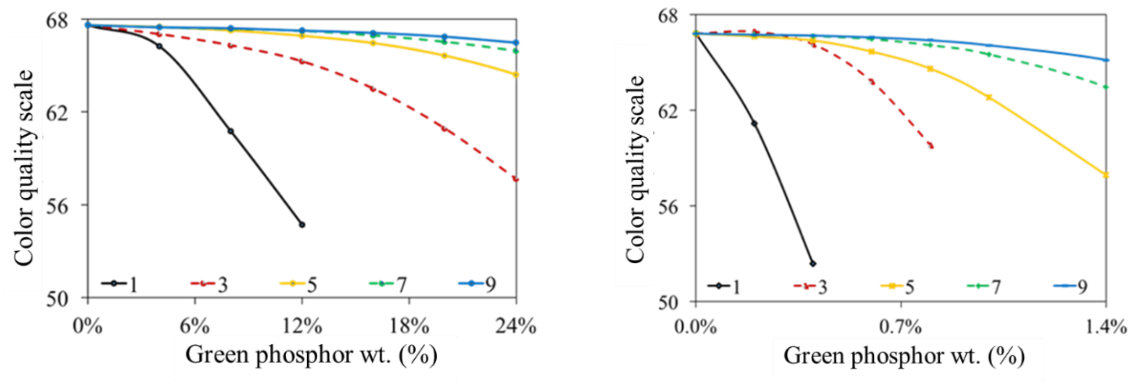

(a) (b)

Figure 6. Hue standard scale correlating with the dosage as well as magnitude for $ZnB_2O_4:Mn^{2+}$: (a) CP and (b) IP

The luminous productivity develops in lockstep with the dosage of $ZnB_2O_4:Mn^{2+}$, as seen in the simulation in Figure 5(a) to Figure 5(c), while the hue standard scale shows degradation with the presence of this green phosphor, as in Figure 6. However, at the higher $ZnB_2O_4:Mn^{2+}$ concentration, the reduction of CQS is much smaller than that at the lower concentration, see Figure 6(a). Additionally, as demonstrated above, the more elevated the concentration of $ZnB_2O_4:Mn^{2+}$, the lower the color deviations, leading to higher color uniformity, as shown in Figure 6(b). Thus, overall, the rise in the green phosphor $ZnB_2O_4:Mn^{2+}$ amount can be considered as an advantage to the performance quality of the WLEDs.

4. CONCLUSION

This research's primary intention is to show the influence of the green $ZnB_2O_4:Mn^{2+}$ phosphor and its capacity to improve the hue uniformity and luminous productivity of white LED packets. First, if we apply the Mie-scattering theory, color uniformity can somewhat embellish despite the mean CCT factor or phosphor geometry. It occurs as a result of illumination-dispersing compensation in white LED packets. Second, the fluctuation of illumination output is shown to hinge on the $ZnB_2O_4:Mn^{2+}$ dosage utilizing Monte Carlo simulation. The illumination output does indeed rise as the $ZnB_2O_4:Mn^{2+}$ concentration changes.

REFERENCES

[1] M. Talone and G. Zibordi, "Spatial uniformity of the spectral radiance by white LED-based flat-fields," *OSA Continuum*, vol. 3, no. 9, pp. 2501-2511, 2020, doi: 10.1364/OSAC.394805.
[2] W. Zhong, J. Liu, D. Hua, S. Guo, K. Yan, and C. Zhang, "White LED light source radar system for multi-wavelength remote sensing measurement of atmospheric aerosols," *Applied Optics*, vol. 58, no. 31, pp. 8542-8548, 2019, doi: 10.1364/AO.58.008542.
[3] S. Feng and J. Wu, "Color lensless in-line holographic microscope with sunlight illumination for weakly-scattered amplitude objects," *OSA Continuum*, vol. 2, no. 1, pp. 9-16, 2019, doi: 10.1364/OSAC.2.000009.
[4] J. -O Kim, H. -S. Jo, and U. -C. Ryu, "Improving CRI and Scotopic-to-Photopic Ratio Simultaneously by Spectral Combinations of CCT-tunable LED Lighting Composed of Multi-chip LEDs," *Current Optics and Photonics*, vol. 4, no. 3, pp. 247-252, 2020. [Online]. Available: https://opg.optica.org/directpdfaccess/94630eee-6ebe-48a7-a25953cdb63eafc8_433063/copp-4-3-247.pdf?da=1&id=433063&seq=0&mobile=no
[5] Y. Zhou *et al.*, "Comparison of nonlinear equalizers for high-speed visible light communication utilizing silicon substrate phosphorescent white LED," *Optics Express*, vol. 28, no. 2, pp. 2302-2316, 2020, doi: 10.1364/OE.383775.
[6] A. J. Henning, J. Williamson, H. Martin, and X. Jiang, "Improvements to dispersed reference interferometry: beyond the linear approximation," *Applied Optics*, vol. 58, no. 1, pp. 131-136, 2019, doi: 10.1364/AO.58.000131.
[7] N. D. Q. Anh, P. X. Le, and H. -Y. Lee, "Selection of a Remote Phosphor Configuration to Enhance the Color Quality of White LEDs," *Current Optics and Photonics*, vol. 3, no. 1, pp. 78-85, 2019, doi: 10.3807/COPP.2019.3.1.078.
[8] Q. Guo, *et al*., "Characterization of YAG:Ce phosphor dosimeter by the co-precipitation method for radiotherapy," *Applied Optics*, vol. 60, no. 11, pp. 3044-3048, 2021, doi: 10.1364/AO.419800.
[9] R. Deeb, J. V. D. Weijer, D. Muselet, M. Hebert, and A. Tremeau, "Deep spectral reflectance and illuminant estimation from self-interreflections," *Journal of the Optical Society of America. A*, vol. 36, no. 1, pp. 105-114, 2019, doi: 10.1364/JOSAA.36.000105.
[10] F. Brusola, I. Tortajada, I. Lengua, B. Jordá, and G. P. -Fajarnés, "Parametric effects by using the strip-pair comparison method around red CIE color center," *Optics Express*, vol. 28, no. 14, pp. 19966-19977, 2020, doi: 10.1364/OE.395291.
[11] L. Yang, Q. Zhang, F. Li, A. Xie, L. Mao, and J. Ma, "Thermally stable lead-free phosphor in glass enhancement performance of light emitting diodes application," *Applied Optics*, vol. 58, no. 15, pp. 4099-4104, 2019, doi: 10.1364/AO.58.004099.
[12] A. M. Nahavandi, M. Safi, P. Ojaghi, and J. Y. Hardeberg, "LED primary selection algorithms for simulation of CIE standard illuminants," *Optics Express*, vol. 28, no. 23, pp. 34390-34405, 2020, doi: 10.1364/OE.408754.
[13] S. Kumar, M. Mahadevappa, and P. K. Dutta, "Extended light-source-based lensless microscopy using constrained and regularized reconstruction," *Applied Optics*, vol. 58, no. 3, pp. 509-516, 2019, doi: 10.1364/AO.58.000509.

[14] V. -C. Su and C. -C. Gao, "Remote GaN metalens applied to white light-emitting diodes," *Optics Express*, vol. 28, no. 26, pp. 38883-38891, 2020, doi: 10.1364/OE.411525.
[15] F. -B. Chen, K. -L. Chi, W. -Y. Yen, J. -K. Sheu, M. -L. Lee, and J. -W. Shi, "Investigation on Modulation Speed of Photon-Recycling White Light-Emitting Diodes With Vertical-Conduction Structure," *Journal of Lightwave Technology*, vol. 37, no. 4, pp. 1225-1230, 2019, doi: 10.1109/JLT.2018.2890331.
[16] S. Xu *et al*., "Exploration of yellow-emitting phosphors for white LEDs from natural resources," *Applied Optics*, vol. 60, no. 16, pp. 4716-4722, 2021, doi: 10.1364/AO.424108.
[17] F. Jiang *et al.*, "Efficient InGaN-based yellow-light-emitting diodes," *Photonics Research*, vol. 7, no. 2, pp. 144-148, 2019, doi: 10.1364/PRJ.7.000144.
[18] S. Keshri *et al*., "Stacked volume holographic gratings for extending the operational wavelength range in LED and solar applications," *Applied Optics*, vol. 59, no. 8, pp. 2569-2579, 2020, doi: 10.1364/AO.383577.
[19] X. Xi *et al*., "Chip-level Ce:GdYAG ceramic phosphors with excellent chromaticity parameters for high-brightness white LED device," *Optics Express*, vol. 29, no. 8, pp. 11938-11946, 2021, doi: 10.1364/OE.416486.
[20] H. S. El-Ghoroury, Y. Nakajima, M. Yeh, E. Liang, C. -L. Chuang, and J. C. Chen, "Color temperature tunable white light based on monolithic color-tunable light emitting diodes," *Optics Express*, vol. 28, no. 2, pp. 1206-1215, 2020, doi: 10.1364/OE.375320.
[21] P. Zhu, H. Zhu, G. C. Adhikari, and S. Thapa, "Spectral optimization of white light from hybrid metal halide perovskites," *OSA Continuum*, vol. 2, no. 6, pp. 1880-1888, 2019, doi: 10.1364/OSAC.2.001880.
[22] H. Yuce, T. Guner, S. Balci, and M. M. Demir, "Phosphor-based white LED by various glassy particles: control over luminous efficiency," *Optics Letters*, vol. 44, no. 3, pp. 479-482, 2019, doi: 10.1364/OL.44.000479.
[23] Q. Xu, L. Meng, and X. Wang, "Nanocrystal-filled polymer for improving angular color uniformity of phosphor-converted white LEDs," *Applied Optics*, vol. 58, no. 27, pp. 7649-7654, 2019, doi: 10.1364/AO.58.007649.
[24] J. Chen, B. Fritz, G. Liang, X. Ding, U. Lemmer, and G. Gomard, "Microlens arrays with adjustable aspect ratio fabricated by electrowetting and their application to correlated color temperature tunable light-emitting diodes," *Optics Express*, vol. 27, no. 4, pp. A25-A38, 2019, doi: 10.1364/OE.27.000A25.
[25] G. Zhang, K. Ding, G. He, and P. Zhong, "Spectral optimization of color temperature tunable white LEDs with red LEDs instead of phosphor for an excellent IES color fidelity index," *OSA Continuum*, vol. 2, no. 4, pp. 1056-1064, 2019, doi: 10.1364/OSAC.2.001056.

BIOGRAPHIES OF AUTHORS

Ha Thanh Tung received the PhD degree in physics from University of Science, Vietnam National University Ho Chi Minh City, Vietnam, he is working as a lecturer at the Faculty of Basic Sciences, Vinh Long University of Technology Education, Vietnam. His research interests focus on developing the patterned substrate with micro- and nano-scale to apply for physical and chemical devices such as solar cells, OLED, photoanode. He can be contacted at email: tunghtvlcrdt@gmail.com.

Huu Phuc Dang received a Physics Ph.D degree from the University of Science, Ho Chi Minh City, in 2018. Currently, he is a lecturer at the Faculty of Fundamental Science, Industrial University of Ho Chi Minh City, Ho Chi Minh City, Vietnam. His research interests include simulation LEDs material, renewable energy. He can be contacted at email: danghuuphuc@iuh.edu.vn.